JACS ARTICLES

Published on Web 08/12/2010

Competitive Carbon−Sulfur vs Carbon−Carbon Bond Activation of 2-Cyanothiophene with [Ni(dippe)H]$_2$

Matthew R. Grochowski, Ting Li, William W. Brennessel, and William D. Jones*

Department of Chemistry, University of Rochester, Rochester, New York 14627

Received May 14, 2010; E-mail: jones@chem.rochester.edu

Abstract: The processes of C−C and C−S bond cleavage have been studied with the homogeneous organometallic compound [Ni(dippe)H]$_2$ (**1**). When **1** is reacted with 2-cyanothiophene at room temperature, cleavage of the nitrile-substituted C−S bond occurs, forming the Ni−metallacycle complex (dippe)Ni(κ^2-S,C-SCH═CHCH═C(CN)) (**2a**), which has been fully characterized by NMR spectroscopy and X-ray diffraction. **2a** was converted to the C−CN cleavage product (dippe)Ni(CN)(2-thiophenyl) (**3**) when heated in solution. On closer inspection, four other intermediates were observed by ^{31}P NMR spectroscopy at low temperature. Structures for the intermediates were elucidated through a combination of independent synthesis, theoretical calculations, chemical characterization, and experimental precedent. A kinetic product (dippe)Ni(κ^2-S,C-SC(CN)═CHCH═CH) (**2b**) was formed from cleavage of the nonsubstituted C−S bond, as well as a Ni(0) η^2-nitrile intermediate, (dippe)Ni(η^2-C,N-2-cyanothiophene) (**4**), and a dinuclear mixed Ni(0)−Ni(II) product (**6b**). A complete DFT analysis of this system has been carried out to reveal comparative details about the two bond cleavage transition states.

Introduction

The processing of petroleum represents perhaps the largest scale organic chemical process currently in practice. Two of the most important steps in this processing are catalytic cracking (C−C bond cleavage) and hydrodesulfurization (C−S bond cleavage).[1] The petroleum industry employs large-scale heterogeneous (zeolitic) catalysts for effecting these reactions.[2] Over the past decades, homogeneous transition metal compounds have been studied with the goal of providing fundamental information about these bond-breaking reactions.

Fluid catalytic cracking (FCC) is the most important conversion process used in petroleum refineries. It is widely employed to convert the high-boiling, high-molecular-weight hydrocarbon fractions of petroleum crude oils to more valuable gasoline, olefinic gases, and other products. The zeolite used in FCC catalysts is referred to as faujasite or Type Y, and the catalytic sites are strongly acidic.[3]

Hydrodesulfurization (HDS) is the process by which sulfur is removed from hydrocarbons during the refinement of petroleum. Failure to remove sulfur during this process results in the formation of noxious sulfur oxides upon fuel combustion which are a major cause of air pollution. Current catalyst efficiency must be improved to meet increasingly rigorous environmental standards. The current heterogeneous catalyst that is employed, Ni/Mo (or Mo/Co) sulfide, is effective for removing most organo-sulfur compounds. However, removal of substituted thiophenes remains problematic, and improvement in catalyst efficiency will require increased effectiveness toward these compounds.[4]

Transition metal compounds that cleave C−C bonds in homogeneous solution are relatively limited. General examples that have been established involve energetically favorable reactions that depend on relief of ring strain,[5] attainment of aromaticity,[6] or reduction of entropic factors via intramolecular C−C cleavage.[7] Examples of alkane C−C cleavage by homogeneous metal complexes are rare, although there have been recent reports that take advantage of dehydrogenation/metathesis pathways[8] or metal radical pathways[9] to achieve aliphatic C−C cleavage. Our laboratory has reported sp−sp^2 C−C cleavage in aliphatic,[10] aromatic,[11] and allylic nitriles.[12] In these examples, the complex [Ni(dippe)H]$_2$ (**1**) reacts to form complexes in which the [Ni(dippe)] fragment first coordinates η^2 to the nitrile C≡N (R = alkyl or aryl) or C═C (R = allyl, aryl) moiety. Rearrangement then occurs to give the C−CN oxidative addition

(1) Gary, J. H.; Handwerk, G. E.; Kaiser, M. E. *Petroleum Refining Technology and Economics*, 5th ed.; CRC Press: Boca Raton, 2007. Leffler, W. L. *Petroleum Refining for the Nontechnical Person*, 2nd ed.; PennWell Books: Tulsa, OK, 1985.
(2) Yang, W.-C. *Handbook of Fluidization and Fluid Particle Systems*; CRC Press: Boca Raton, 2003.
(3) (a) Gary, J. H.; Handwerk, G. E. *Petroleum Refining: Technology and Economics*, 4th ed.; CRC Press: Boca Raton, 2001. Speight, J. G. *The Chemistry and Technology of Petroleum*, 4th ed.; CRC Press: Boca Raton, 2006. Sadeghbeigi, R. *Fluid Catalytic Cracking Handbook*, 2nd ed.; Gulf Publishing: , 2000.
(4) Topsoe, H.; Clausen, B. S.; Massoth, F. E. *Hydrotreating Catalysis*; Springer: Berlin, 1996.
(5) Adams, D. M.; Chatt, J.; Guy, R. G.; Sheppard, N. *J. Chem. Soc.* **1961**, 738–742. Steffen, A.; Ward, R. M.; Jones, W. D.; Marder, T. B. *Coord. Chem. Rev.* **2010**, *254*,in press.
(6) Benfield, F. W. C.; Green, M. L. H. *J. Chem. Soc., Dalton Trans.* **1974**, 1324.
(7) Suggs, J. W.; Jun, C.-H. *J. Chem. Soc., Chem. Commun.* **1985**, 92. Gozin, M.; Aizenberg, M.; Liou, S.-Y.; Weisman, A.; Ben-David, Y.; Milstein, D. *Nature* **1994**, *370*, 42.
(8) Goldman, A. S.; Roy, A. H.; Huang, Z.; Ahuja, R.; Schinski, W.; Brookhart, M. *Science* **2006**, *312*, 257.
(9) Chan, Y. W.; Chan, K. S. *J. Am. Chem. Soc.* **2010**, *132*, 6920.
(10) (a) García, J. J.; Arévalo, A.; Brunkan, N. M.; Jones, W. D. *Organometallics* **2004**, *23*, 3997. (b) Ateşin, T. A.; Li, T.; Lachaize, S.; Brennessel, W. W.; García, J. J.; Jones, W. D. *J. Am. Chem. Soc.* **2007**, *129*, 7562.

 10.1021/ja104158h

product Ni(dippe)(R)(CN). One case studied in detail was the cleavage of the C−CN bond in benzonitrile, which occurs via reversible rearrangement to an η^2-C,C complex prior to C−C cleavage (eq 1).

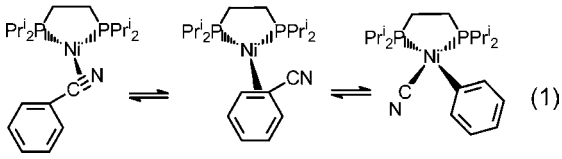

(1)

Many homogeneous organometallic systems have also been studied in an attempt to better understand the mechanism(s) of HDS,[13] including model studies of C−S cleavage at Mo,[14] Co,[15] Rh,[16] Ir,[17] and Pt.[18] The complex [Ni(dippe)H]$_2$ (**1**) has also been found to insert into the C−S bonds of a wide range of thiophenes, including the challenging dibenzothiophene, 4-methyldibenzothiophene, and 4,6-dimethyldibenzothiophene substrates.[19] The reaction of thiophene with **1** is shown in eq 2, where the product (dippe)Ni(κ^2-C,S-C$_4$H$_4$S) is typical of the C−S insertion that takes place. **1** undergoes loss of H_2 when

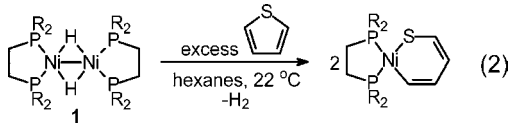

1 (2)

reacted with a substrate to produce the highly reactive 14-electron Ni(0)-dippe fragment bound to the substrate, which then continues on to a Ni(II) d^8 square planar product.[19b] Interestingly, while (dippe)Ni(κ^2-C,S-C$_4$H$_4$S) is stable under nitrogen in the solid state, it forms an equilibrium with a dinuclear complex if it is left in THF solution (eq 3), indicating *reversible* C−S bond cleavage. Reaction of **1** with dibenzothiophene gives the analogous (dippe)Ni(κ^2-C,S-C$_{12}$H$_8$S)], which undergoes desulfurization to give four unique products.[19b]

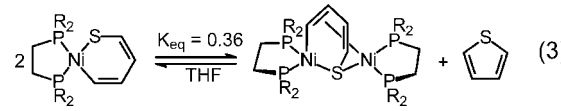

(3)

This work specifically addresses the reaction of **1** with 2-cyanothiophene, where the possibility for C−CN cleavage exists in competition with the various C−S cleavage reactions. Reaction of 2-cyanothiophene with the platinum analogue [Pt(dippe)] has already been examined.[20] The Pt(dippe) fragment was found to cleave both the nitrile-substituted and unsubstituted C−S bonds. Cleavage away from the cyano group was preferred kinetically, while cleavage adjacent to the cyano group was thermodynamically preferred (eq 4). No C−CN cleavage was

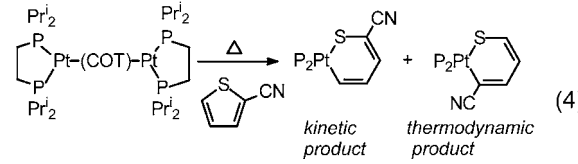

(4)

observed, even after heating the sample at 160 °C for several months. The reaction was also studied using density functional theory (B3LYP), and the theoretical calculations were found to be useful for comparing transition states for the two types of bond cleavage. The work presented here compares experimental and computational results, and shows marked differences with the platinum system.

Results and Discussion

Reaction of 1 with 2-Cyanothiophene. The reaction of **1** with 2-cyanothiophene occurred cleanly and rapidly at room temperature in THF to give the C−S insertion complex (dippe)Ni(κ^2-S,C-SCH=CHCH=C(CN)) (**2a**) in 93% isolated yield (eq 5). The insertion occurred exclusively at the *substituted* C−S

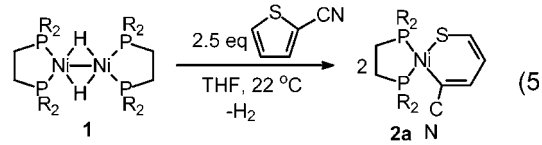

1 **2a** (5)

bond. The ^{31}P NMR spectrum showed two closely spaced doublets at δ 73.06 and 72.22 that resemble a virtual quartet (J_{P-P} = 34 Hz). Orange block crystals suitable for X-ray diffraction were grown from a layered solution of benzene/hexanes at −30 °C. The crystal structure in Figure 1 shows a nickel metallacycle product with a square planar geometry around the Ni(II) center. The bond lengths and angles are very

(11) (a) Garcia, J. J.; Jones, W. D. *Organometallics* **2000**, *19*, 5544. (b) Garcia, J. J.; Brunkan, N. M.; Jones, W. D. *J. Am. Chem. Soc.* **2002**, *124*, 9547. (c) Atesin, T. A.; Li, T.; Lachaize, S.; Brennessel, W. W.; García, J. J.; Jones, W. D. *Organometallics* **2008**, *27*, 3811. (d) Li, T.; García, J. J.; Brennessel, W. W.; Jones, W. D. *Organometallics* **2010**, *29*, 2430.

(12) Acosta-Ramírez, A.; Muñoz-Hernández, M.; Jones, W. D.; García, J. J. *J. Organomet. Chem.* **2006**, *691*, 3895. Acosta-Ramírez, A.; Flores-Gaspar, A.; Muñoz-Hernández, M.; Arévalo, A.; Jones, W. D.; García, J. J. *Organometallics* **2007**, *26*, 1712. Acosta-Ramírez, A.; Muñoz-Hernández, M.; Jones, W. D.; García, J. J. *Organometallics* **2007**, *26*, 5766. Acosta-Ramírez, A.; Flores-Álamo, M.; Jones, W. D.; García, J. J. *Organometallics* **2008**, *27*, 1834. Acosta-Ramírez, A.; Morales-Morales, D.; Serrano-Becerra, J. M.; Arévalo, A.; Jones, W. D.; García, J. J. *J. Mol. Catal. A, Chem.* **2008**, *288*, 14. Swartz, B. D.; Reinartz, N. M.; Garcia, J. J.; Jones, W. D. *J. Am. Chem. Soc.* **2008**, *130*, 8548. See also: Van der Vlugt, J. I.; Hewat, A. C.; Neto, S.; Sablong, R.; Mills, A. M.; Lutz, M.; Spek, A. L.; Müller, C.; Vogt, D. *Adv. Synth. Catal.* **2004**, *346*, 993. Wilting, J.; Muller, C.; Hewat, A. C.; Ellis, D. D.; Tooke, D. M.; Spek, A. L.; Vogt, D. *Organometallics* **2005**, *24*, 13. Chaumonnot, A.; Lamy, F.; Sabo-Etienne, S.; Donnadieu, B.; Chaudret, B.; Barthelat, J. C.; Galland, J. C. *Organometallics* **2004**, *23*, 3363.

(13) Sanchez-Delgado, R. A. *Organometallic Modelling of the Hydrodesulphurization and Hydronitrogenation Reactions*; Kluwer Academic Publishers: Dordrecht, 2002.

(14) Churchill, D. G.; Bridgewater, B. M.; Parkin, G. *J. Am. Chem. Soc.* **2000**, *122*, 178.

(15) Jones, W. D.; Chin, R. M. *Organometallics* **1992**, *11*, 2698.

(16) Myers, A. W.; Jones, W. D. *Organometallics* **1996**, *15*, 2905. Paneque, M.; Taboada, S.; Carmona, E. *Organometallics* **1996**, *15*, 2678.

(17) Selnau, H. E.; Merola, J. S. *Organometallics* **1993**, *12*, 1583. Bianchini, C.; Meli, A.; Peruzzini, M.; Vizza, F.; Frediani, P.; Herrera, V.; Sánchez-Delgado, R. A. *J. Am. Chem. Soc.* **1993**, *115*, 2731. Jones, W. D.; Chin, R. M. *J. Am. Chem. Soc.* **1994**, *116*, 198. (c) Bianchini, C.; Jimenez, V.; Meli, A.; Vizza, F.; Herrera, V.; Sánchez-Delgado, R. A. *Organometallics* **1995**, *14*, 2342. Paz-Sandoval, M. A.; Cervantes-Vasquez, M.; Young, V. M., Jr.; Guzei, I. A.; Angelici, R. J. *Organometallics* **2004**, *23*, 1274.

(18) García, J.; Maitlis, P. M. *J. Am. Chem. Soc.* **1993**, *115*, 12200. García, J.; Mann, B. E.; Adams, H.; Bailey, N. A.; Maitlis, P. M. *J. Am. Chem. Soc.* **1995**, *117*, 2179. (b) Iretskii, A.; Adams, H.; García, J. J.; Maitlis, P. M. *J. Chem. Soc., Chem. Commun.* **1998**, 61. Arévalo, A.; Bernès, S.; García, J. J.; Picazo, G.; Maitlis, P. M. *Organometallics* **1999**, *18*, 1680.

(19) (a) Vicic, D. A.; Jones, W. D. *J. Am. Chem. Soc.* **1997**, *119*, 10855. (b) David, A. Vicic.; William, D. Jones. *J. Am. Chem. Soc.* **1999**, *121*, 7606. (c) Vicic, D. A.; Jones, W. D. *Organometallics* **1998**, *17*, 3411.

(20) Ateşin, T. A.; Ateşin, A. C.; Skugrud, K.; Jones, W. D. *Inorg. Chem.* **2008**, *47*, 4596.

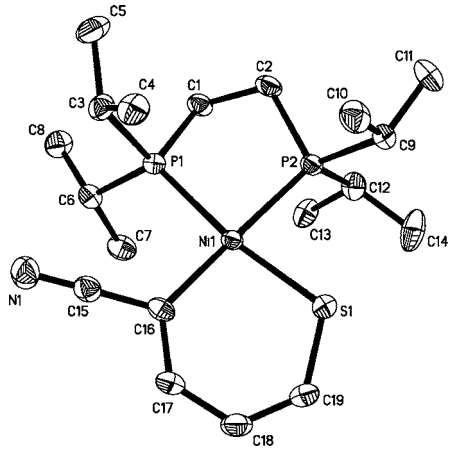

Figure 1. Crystal structure of [(dippe)Ni(η^2-C,S-2-cyanothiophene)] (**2a**). Ellipsoids are shown at the 50% probability level. Selected bond lengths (Å): Ni(1)−C(16), 1.9351(17); Ni(1)−S(1), 2.1590(5); Ni(1)−P(1), 2.2211(5); Ni(1)−P(2), 2.2238(5); C(16)−C(17), 1.384(2); C(17)−C(18), 1.415(3); C(18)−C(19), 1.349(3); C(19)−S(1), 1.702(2). Selected bond angles (°): S(1)−Ni(1)−C(16), 94.44(6); P(2)−Ni(1)−S(1), 83.955(19); P(2)−Ni(1)−P(1), 86.398(18); P(1)−Ni(1)−C(16), 95.29(6).

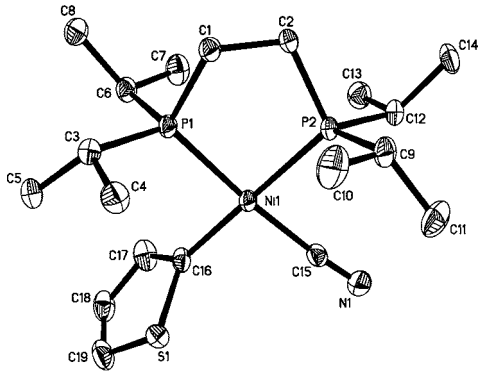

Figure 2. Crystal structure of (dippe)Ni(2-thienyl)(CN) (**3**). Ellipsoids are shown at the 50% probability level. Selected bond lengths (Å): Ni(1)−C(16), 1.918(3); Ni(1)−C15, 1.877(2); Ni(1)−P(1), 2.1730(7); Ni(1)−P(2), 2.1821(7); C(16)−C(17), 1.373(13); C(17)−C(18), 1.397(15); C(18)−C(19), 1.342(6); C(19)−S(1), 1.737(5); S(1)−C(16), 1.729(7); C(15)−N(1), 1.137(3). Selected bond angles (°): P(1)−Ni(1)−P(2), 88.49(3); P(1)−Ni(1)−C(16), 92.3(4); C(16)−Ni(1)−C(15), 90.6(4); P(2)−Ni(1)−C(15), 88.48(7).

similar to those of (dippe)Ni(κ^2-C,S-C_4H_4S). **2a** was isolated as a solid that is stable under nitrogen. Exposure to air caused the compound to decompose, and dippe oxide could be observed by ^{31}P NMR spectroscopy (δ 52.9, THF). When **2a** was heated in THF at 85 °C over a period of 13 h, transformation of the compound occurred to give the C−CN bond-activated product (dippe)Ni(CN)(2-thiophene) (**3**) (eq 6). Over the course of the

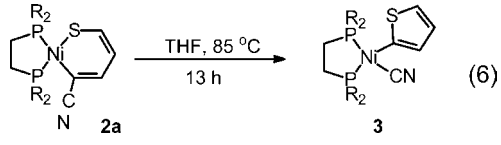

(6)

reaction, some Ni(dippe)$(CN)_2$ precipitated out of solution as a byproduct,[10a] and doublet resonances for **3** were observed at δ 85.64 and 76.89 (J_{P-P} = 31 Hz). The isolated product (74%) was crystallized from benzene/hexanes, and X-ray diffraction was used to obtain a crystal structure of **3** (Figure 2), showing the expected square planar geometry around the nickel center,

Scheme 1

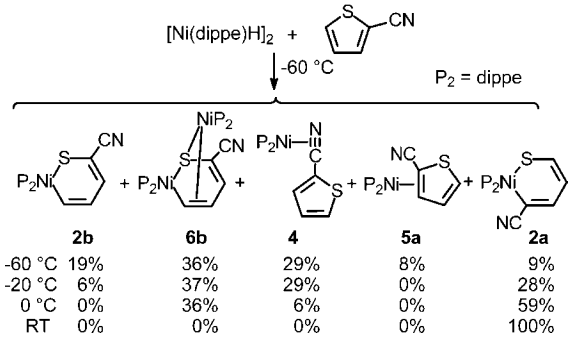

	2b	**6b**	**4**	**5a**	**2a**
-60 °C	19%	36%	29%	8%	9%
-20 °C	6%	37%	29%	0%	28%
0 °C	0%	36%	6%	0%	59%
RT	0%	0%	0%	0%	100%

with thiophene perpendicular to the plane. The Ni−P bond lengths of 2.17 Å are slightly shorter than the 2.22 Å found for **2a**.

Observation of Intermediates at Low Temperature. No intermediates in the reaction of **1** with 2-cyanothiophene were readily apparent at room temperature due to the rapidity of the reaction. When 4 equiv of 2-cyanothiophene was added to a solution of **1** at −60 °C in THF-d_8, however, several intermediates were observed while monitoring the reaction by ^{31}P NMR spectroscopy, as summarized in Scheme 1. **2a** was present but in a small proportion (9%) compared to the other species. A direct relationship between the P−P coupling constant and the nickel oxidation state has been noted in previous studies of reactions involving **1**.[11b] In these studies, a Ni(0) complex is typified by a P−P coupling constant of J > 60 Hz, while Ni(II) complexes are typified by J < 40 Hz. In addition to the small quantity of **2a**, a second Ni(II) complex was present (19%) with doublet resonances at δ 85.29 and 74.29 (J_{P-P} = 23 Hz). This product appears to be the C−S-activated complex arising from insertion into the nonsubstituted C−S bond, (dippe)Ni(κ^2-S,C-SC(CN)═CHCH═CH) (**2b**). Theoretical calculations lend support to this assignment (vide infra). NMR integration showed the ratio of **2b**:**2a** at −60 °C to be 2:1. This observation parallels the reaction involving the Pt−dippe analogue, in which activation of the nonsubstituted C−S bond of 2-cyanothiophene is observed as a kinetic product, with eventual conversion to the thermodynamically favored activation of the nitrile-substituted C−S bond.[20]

Two Ni(0) products were present, one displaying a pair of doublets at δ 79.99 and 68.73 (J_{P-P} = 62 Hz) (**4**) and a second displaying a set of doublets at δ 64.16 and 60.03 (J_{P-P} = 75 Hz) (**5a**). **4** was a major component of the mixture (29%) and is proposed to be (dippe)Ni(η^2-C,N-2-cyanothiophene) (Scheme 1). This complex was fairly stable and did not disappear until the reaction temperature was raised to 0 °C (Figure 3). Theoretical calculations (vide infra) and experimental precedent were used in the assignment of this structure. Previously, when **1** was reacted with 2-cyanopyridine, the η^2(C,N) complex formed and was structurally characterized.[21] The ^{31}P NMR data showed doublets at δ 82.3 and 68.6 (J_{P-P} = 68 Hz), very similar to those found for **4**. A previous study of the reaction with benzonitrile showed formation of an η^2(C,N) complex that was structurally characterized and which showed doublet resonances at δ 78.6 and 66.4 (J_{P-P} = 68 Hz) in the ^{31}P NMR spectrum.[22] Both of these reactions also went on to give their respective C−CN activated products. The 2-cyanothiophene reaction

(21) Garcia, J. J.; Brunkan, N. M.; Jones, W. D. *J. Am. Chem. Soc.* **2002**, *124*, 9547.
(22) Garcia, J. J.; Jones, W. D. *Organometallics* **2000**, *19*, 5544.

therefore has a reaction pathway similar to those of 2-cyanopyridine[11b] and benzonitrile,[11] although **4** is more transient than the other previously studied η^2(C,N) species. **5a** was a short-lived Ni(0) intermediate that disappeared after 10 min at −60 °C; it was assigned to the η^2-C,C adduct.

Another major component of the mixture that was observed in the NMR spectrum had broad resonances present at δ 69.27 and 61.46. As the reaction temperature was increased, the resonances became narrower and splitting was then observed (J_{P-P} = 17 Hz). This complex is assigned as the dinuclear complex [(dippe)Ni]$_2$(μ-κ^2:η^3-1-cyanobutadienylthiolate) (**6b**), analogous to the known fluxional parent complex without a cyano group (eq 3).[19b] Further evidence for assignment of this structure as being derived from the kinetic insertion product **2b** is described below.

6b was quite stable, based upon its persistent presence in the ^{31}P NMR spectra (Scheme 1, Figure 3). **6b** formed at −60 °C and was unreactive until it was the only product present besides **2a** at 0 °C. Compounds **2a**, **2b**, **4**, and **6b** apparently form a steady-state equilibrium at −60 °C, as their relative concentrations rapidly stabilize. When the reaction was warmed to −20 °C, **2b** was consumed while **2a** grew in. There was a small decrease in **4** and no change in **6b**. The reaction was then warmed to 0 °C, whereupon **2b** was consumed immediately while **4** began to be rapidly consumed as **2a** grew in proportionally. **6b** did not change its percent composition after 95 min at 0 °C, and if only 1 equiv of 2-cyanothiophene is employed per two Ni(dippe) fragments, **6b** is stable at room temperature for days. As the reaction was warmed to room temperature, **6b** reacted with excess 2-cyanothiophene to give **2a** as the only product.

Evidence for a Binuclear Intermediate 6b. The identity of **6b** was established primarily by independent synthesis. It was first thought that **6b** may have been **2b**, given its small P−P coupling constant (J = 17 Hz). To explore this possibility, **1** was reacted with 2,5-dicyanothiophene, since cleavage of either C−S bond would give the same product. When the reaction was performed at room temperature, a long-lived intermediate (**6c**) was seen with broad resonances at δ 69.05 and 58.98 that were very similar to those observed for **6b** (eq 7). The final

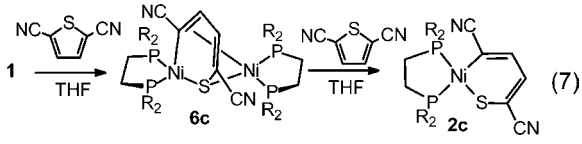

product was the C−S insertion product (dippe)Ni(κ^2-S,C-1,4-dicyanobutadienylthiolate)] (**2c**), with a virtual quartet centered at δ 76.17 (J_{P-P} = 37 Hz). X-ray diffraction was employed to confirm its structure, which is similar to that of **2a**, with square planar geometry around Ni and nearly identical bond lengths and angles (Figure 4).

The ^{1}H NMR spectrum of **6c** supports the proposed dinuclear structure of the nickel(II) butadienethiolate metallacycle coordinated to a Ni(0)-dippe fragment. The two butadienyl resonances were observed at δ 4.94 and 7.80, the upfield shift being indicative of π-coordination to a Ni(0) center. The ^{13}C NMR spectrum also demonstrated this phenomenon, with two of the butadienethiolate resonances shifted upfield to δ 99.36 and 77.77, compared to the corresponding resonances in **2c**, where the farthest upfield vinylic carbon peaks occurred at δ 111. **6c** is a black solid formed in quantitative yield, and its composition was confirmed by elemental analysis. Chemical characterization

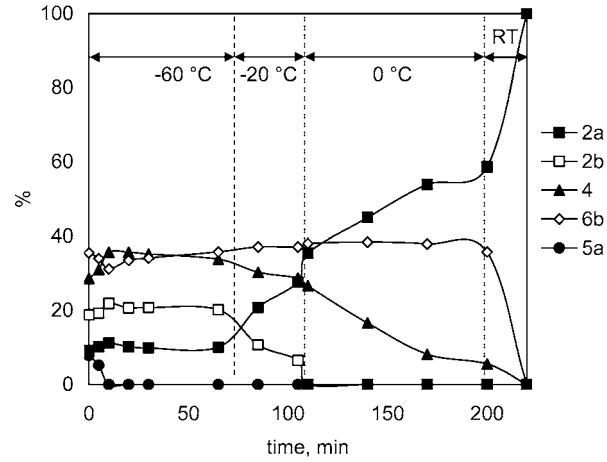

Figure 3. Temperature dependence of the intermediates in Scheme 1.

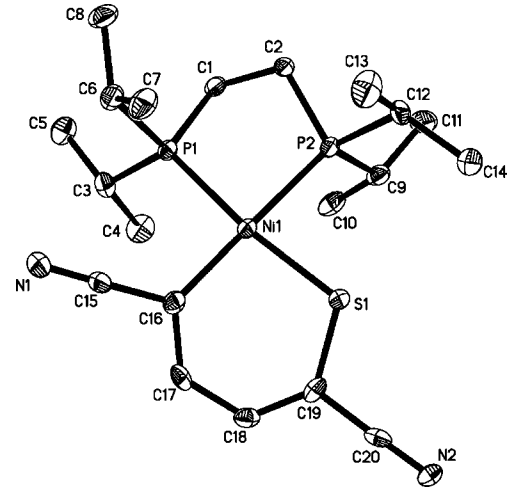

Figure 4. Crystal structure of (dippe)Ni(η^2-C,S-1,4-dicyanobutadienylthiolate) (**2c**). Ellipsoids are shown at the 50% probability level. Selected bond lengths (Å): Ni(1)−C(16), 1.926(5); Ni(1)−S(1), 2.1444(16); Ni(1)−P(1), 2.2005(16); Ni(1)−P(2), 2.2270(16). Selected bond angles (°): S(1)−Ni(1)−C(16), 94.73(17); P(2)−Ni(1)−S(1), 84.60(6); P(2)−Ni(1)−P(1), 86.88(6); P(1)−Ni(1)−C(16), 93.74(17).

was also carried out by reacting **6c** with a stoichiometric amount of chloroform. The chloroform acted as a quenching agent and gave **2c** and Ni(dippe)Cl$_2$. These products are consistent with the proposed structure for **6c** in which the coordinating Ni^0(dippe) fragment is converted to Ni^{II}(dippe)Cl$_2$.

Independent synthesis of **6b** proved to be more challenging than that of **6c**. Reaction of **2a** with excess **1** (0.75 equiv) gave **6b**, as seen in the low-temperature reaction, but also gave an additional product (**6a**) with a pair of broad resonances in the ^{31}P NMR spectrum (eq 8). The two sets of peaks were proposed

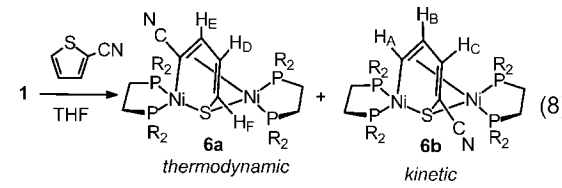

to correspond to isomeric dinuclear compounds, **6a** and **6b**, in a 3:1 ratio. A corresponding set of ^{1}H NMR resonances was seen for each product with the same 3:1 ratio (Figure 5).

^{1}H NMR resonances for the butadienylthiolate protons of **6b** were observed at δ 4.76, 5.68, and 7.51 in both the low-

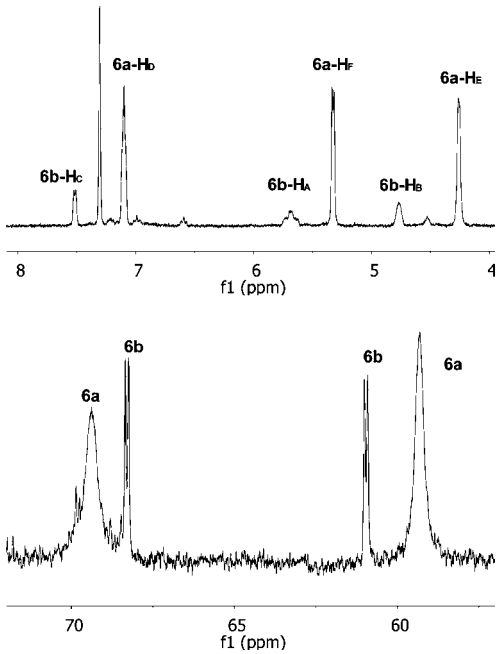

Figure 5. (Top) ^{1}H NMR spectrum of thienyl peaks for eq 8. (Bottom) ^{31}P NMR of dippe peaks for eq 8. THF-d_8, 25 °C.

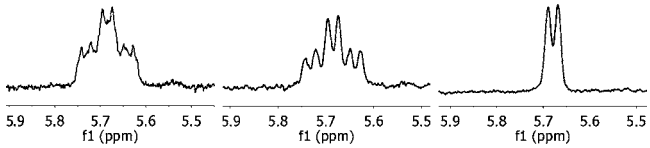

Figure 6. (Left) **6b**-H_A before decoupling. (Middle) Irradiation of **6b**-P_A nuclei at δ 68.38 results in resolution to a triplet of doublets. (Right) Broadband ^{1}H{^{31}P} resolves **6b**-H_A to a doublet.

temperature reaction of **1** with 2-cyanothiophene and the independent synthesis described above, where it appeared to be the *minor* product. Similar resonances were observed for **6a** at δ 4.25, 5.35, and 7.08. Identification and differentiation of **6b** and **6a** were made on the basis of the splitting patterns of the resonances. For **6b**, complex patterns were observed at δ 4.76 (H_B) and especially δ 5.68 (H_A), while splitting patterns for **6a** were simpler. The proposed structure for **6b** would allow for coupling between phosphorus nuclei and the thienyl protons, while such coupling would be largely absent for **6a** due to a larger through-bond distance between the nuclei. Additional support for the assignment of **6a** and **6b** came from reaction of the mixture with chloroform at room temperature, which led to the formation of **2b** and Ni(dippe)Cl_2, similar to the reaction of **6c**.

A series of ^{1}H{^{31}P} decoupling experiments supports the assigned structures. Irradiation of the ^{31}P resonance at δ 68.38 (**6b**-P_A) resulted in resolution of the peak at 5.68 (**6b**-H_A) into a triplet of doublets (Figure 6). Splitting by the two equivalent P_A nuclei gave a triplet ($^3J_{P-H}$ = 18 Hz), which was further split into a doublet (J_{H-H} = 8 Hz) by the adjacent vicinal proton at δ 4.76 (**6b**-H_B). Irradiation of the second ^{31}P resonance of **6b** (P_B) at δ 60.99 resulted in **6b**-H_A being observed as a rounded peak, implying that the set of P_B nuclei gives some residual splitting to H_A. H_B resolved to a triplet, implying residual coupling with P_B nuclei splitting by each of the two adjacent thienyl protons. The doublet at 7.51 (**6b**-H_C) was not affected by ^{1}H{^{31}P} decoupling and was observed as a doublet. A broadband ^{1}H{^{31}P} decoupling experiment showed the following splittings for **6b**: H_A (doublet), H_B (triplet), and H_C (doublet). A COSY NMR spectrum showed that H_A was coupled to H_B, and H_B was coupled to H_A and H_C, while H_C was coupled to H_B. The agreement of the ^{1}H{^{31}P} experiments and COSY experiments supports the proposed structure of **6b**. A COSY spectrum of **6a** showed that the triplet resonance at δ 7.08 (H_D) was coupled to the peak at δ 4.25 (H_E, doublet) and the peak at δ 5.35 (H_F, doublet). The splittings of H_D and H_F were invariant with all attempted ^{1}H{^{31}P} decoupling experiments. A very slight change was seen for H_E, which was tentatively assigned to the resonance at δ 4.25.

A dramatic difference between **6b** and **6a** is the shape of the resonances in the ^{31}P NMR spectrum. **6a** showed resonances that were much broader than those of **6b**, although the chemical shifts were similar. Fluxional exchange is slower in **6a** as compared to **6b**, which accounts for the broadness of the resonances. When a solution containing **6a** was cooled to −40 °C, the two resonances were observed as four broad resonances, consistent with the freezing out of the fluxional process (as seen in the parent complex with thiophene[19b]) and indicative of the low symmetry of **6a** (eq 9). The position of the cyano group

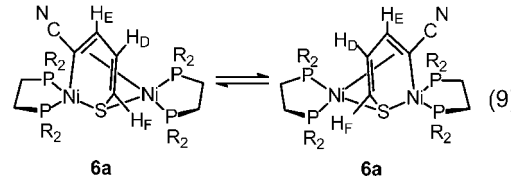

for each isomer may account for the exchange rate differences between **6b** and **6a**; i.e., **6a**, with a cyano substituent on the double bond π-bound to Ni(0), is less labile and its static structure can be frozen out. In addition, the cyano group stabilizes **2b** over **6b** plus 2-cyanothiophene, in contrast to the parent thiophene insertion complex, which establishes an equilibrium between the mononuclear complex and dinuclear complex plus thiophene.[19b]

Computational Studies: Ground States and Transition States. As described above, the low-temperature reaction of [(dippe)NiH]$_2$ with 2-cyanothiophene formed five different complexes, including two C−S activation products. When the same reaction was conducted at 85 °C, only the C−CN cleavage product was observed. On the basis of the experimental results, a computational study was undertaken to examine the energetics and reaction pathways leading to both C−S and C−CN oxidative addition products. To simplify the calculation, the [Ni(dmpe)] fragment was used as a model of the active species [Ni(dippe)], with methyl groups replacing the isopropyl groups.[23] Initially, Ni(dmpe)(2-thienyl)(CN) (**S3**) and Ni(dippe)[κ^2-C,S-SCHCHCHC(CN)] (**S2a**) were constructed on the basis of the X-ray crystallographic structures of **3** and **2a** (Figures 1 and 2), and local minima were found in gas phase calculations.

Both of the optimized structures of **S3** and **S2a** have nearly square planar geometries around nickel coordination sites. The Ni−CN and Ni−C(thiophene) distances in **S3** are 1.868 and 1.915 Å, respectively, similar to those in the crystal structure of **3** (1.877 and 1.918 Å). In **S2a**, the Ni−S bond is 2.195 Å, only 0.036 Å longer than that in the crystal structure of **2a**.

(23) Atesin, T. A.; Li, T.; Jones, W. D. *J. Am. Soc. Chem.* **2007**, *129*, 7562.

Table 1. Optimized Structures (Interatomic Distances in Å, Angles in Deg) and Relative Free Energies (ΔG Relative to Fragments, kcal/mol, PCM-Corrected in THF) of Stationary Points on the [Ni(dmpe)] + 2-cyanothiophene Potential Energy Surface[a]

	Ni−S	Ni−C1	Ni−C2	Ni−C3	Ni−C4	Ni−CN	Ni−N	C−CN	C−N	C1−S	C4−S	α	β	ΔG
S2a	2.195	1.929						1.424	1.172		1.729	13.8	18.9	−50.36
S2b	2.174				1.890			1.430	1.166	1.751		3.7		−44.06
S3		1.915				1.868			1.171	1.755	1.748	78.9	1.4	−44.3
S4						1.872	1.898	1.441	1.238	1.763	1.735	1.4	1.6	−38.88
S5a		1.956	1.977					1.425	1.169	1.822	1.766	66.1		−33.57
S5b				2.000	1.946			1.414	1.167	1.783	1.810	73.0		−32.04
S7a	2.231	1.998						1.428	1.169	1.908	1.743	60.2		−18.7
S7b	2.280				1.960			1.401	1.171	1.771	1.807	76.4		−25.09
TS2a5a	2.214	1.959						1.426	1.169	2.001	1.738	64.6		−19.84
TS2b7b	2.187				1.907			1.413	1.169	1.773	2.179	64.8		−22.47
TS35a		1.967				1.883		1.561	1.19	1.78	1.739	74.6	34.9	−12.09
TS45a		2.427				2.003	2.366	1.412	1.188	1.766	1.746	88.3	62.8	−7.15
TS5a5b		2.293	2.046	2.090	2.309			1.412	1.169	1.813	1.787	87.7		−20.71
TS5b7b	2.346			2.562	1.928			1.402	1.171	1.777	1.802	83.8		−24.15

[a] α is the angle between P−Ni−P and thiophene planes. β is the angle between P−Ni−P and Ni−C−CN planes. The numbering of carbon atoms on the thiophene ring is shown in the thiophene fragment (first structure) in Figure 7 or Figure 11.

With the simplified model, the DFT optimized structures are still consistent with the crystallographic data for the analogous dippe compounds.

The other possible C−S activation product in which cleavage occurs away from the cyano substituent was not stable enough to be isolated. Consequently, the model complex **S2b** was constructed starting from the crystal structure of **2a** and optimized also as a ground state. The transition states leading to the three oxidative addition products **S3**, **S2a**, and **S2b** were located from relaxed potential energy surface scans by constraining the C−S or C−CN distance in the products and optimizing the resulting structures during the processes. Those structures around the energy maxima were optimized as transition states, and the intrinsic reaction coordinate (IRC) routes were calculated in both forward and reverse directions toward the corresponding local minima. The transition state **TS35a** connects the C−CN cleavage product **S3** to a complex **S5a** with nickel η^2-coordinated through the C═C of the thiophene ring next to the CN substituent. The carbon−carbon bond distance is lengthened to 1.458 Å due to back-donation from the nickel center. In the same way, **TS2a5a** was found to connect one of the C−S activation products **S2a** also to **S5a**. **TS2b7b**, on the other hand, connects the other C−S activation product **S2b** to a complex **S7b**, in which the nickel metal coordinates to the C−S bond (a shallow minimum). The C−S distance is elongated from 1.807 Å in **S7b** to 2.179 Å in **TS2b7b**. When further constraining the C−S distance in **S7b**, another transition state, **TS5b7b**, was found. It connects **S7b** to another local minimum, **S5b**, that has nickel η^2-coordinated to the C═C of the thiophene ring away from the CN substitute, similar to **S5a**. Complex **S7a**, the counterpart of **S7b** in the other C−S activation, is slightly higher in energy than **TS2a5a** and therefore was excluded from the C−S activation pathway leading to **S2a**. The nickel metal can also migrate from **S5a** to **S5b** via an η^4-coordinated transition state, **TS5a5b**, which makes possible the intramolecular interchange between the two C−S activation products. All of the optimizations and potential energy surface scans were conducted in the gas phase. Solvent effects on the relative stabilities of all structures were taken into consideration by applying a polarizable continuum model (PCM) correction. The optimized structural parameters and relative energies in THF of all ground states and transition states found in this study are summarized in Table 1 and Figure 7 (see movies for IRC paths in Supporting Information).

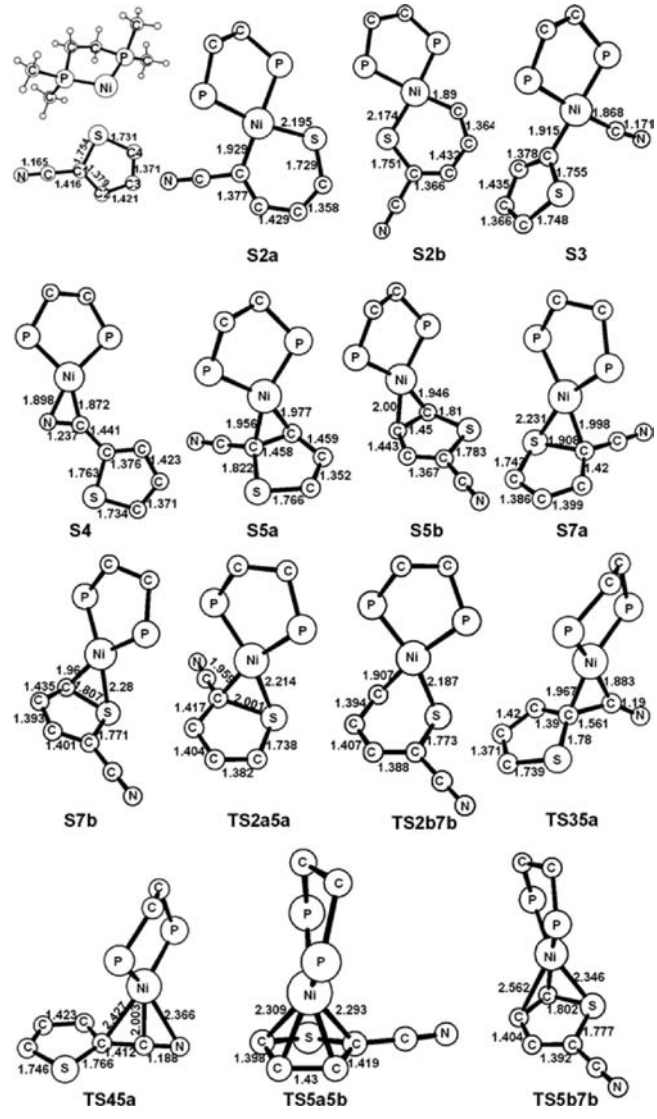

Figure 7. Optimized structures (interatomic distances in Å, angles in deg) of stationary points and transition states on the [Ni(dmpe)] + 2-cyanothiophene potential energy surface. Hydrogen atoms and methyl groups on the phosphorus have been omitted.

Kinetic and Thermodynamic C−S Activations. From the experimental observations, the C−S activation product **2a** is thermodynamically more stable than **2b**. From DFT calculations

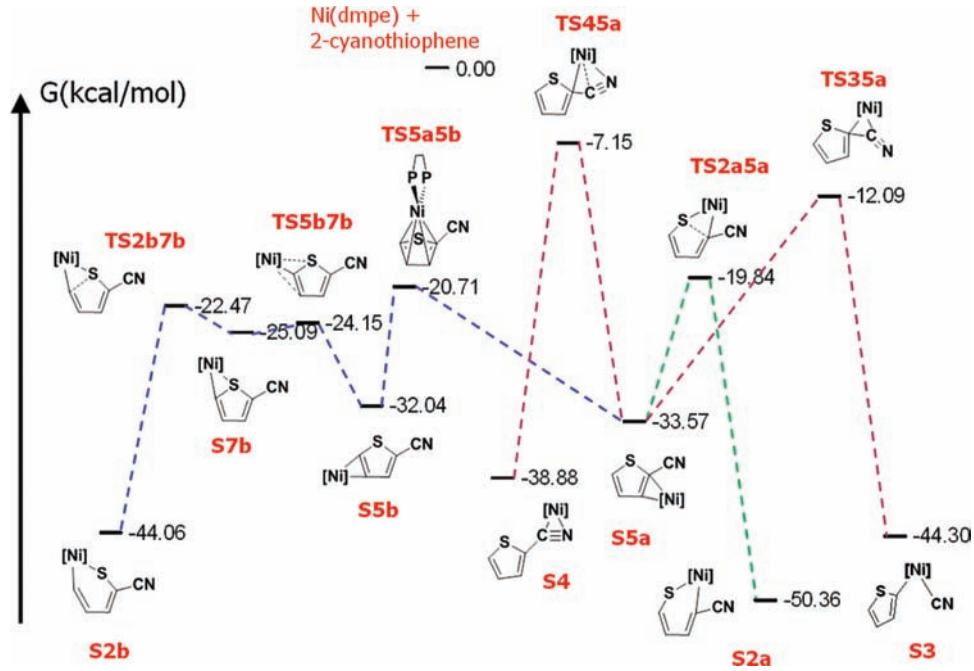

Figure 8. Total free energies (PCM-corrected in THF).

(PCM corrected in THF) as shown in Figure 8, **S2a** lies 6.3 kcal/mol lower in energy than **S2b**. When changing the Ni(dmpe) to the Ni(dippe) fragment, DFT calculations showed that **2a** is still about 3 kcal/mol downhill from **2b**. In agreement, at room temperature, no resonances for **2b** could be seen in the NMR spectrum. On the other hand, from the η^2-C,C-2-cyanothiophene complexes, the activation barrier for the C−S activation leading to **S2a** is 13.7 kcal/mol, and that leading to **S2b** is only 9.6 kcal/mol. Therefore, the calculations are in agreement with the experimental results that **S2b** is the kinetic product while **S2a** is the thermodynamic product. This also matches the previous results obtained with Pt(dmpe) and 2-cyanothiophene,[20] in which a kinetic preference for cleavage of the unsubstituted C−S bond was observed.

C−S vs C−CN Activations. Upon heating, the C−S activation product **2a** converted completely to the C−CN oxidative addition product **3**. When the system was cooled back to room temperature, **2a** was not formed again, indicating that **3** is thermodynamically more stable than **2a**. However, the energetic results from DFT calculations for these two complexes contradict this experimental observation. **S3** was found to lie 6.8 kcal/mol higher in energy than **S2a** in the gas phase. Even after using PCM to correct the solvent effects, **S3** was still *higher* in energy than **S2a** by 8 kcal/mol in benzene and 6.1 kcal/mol in THF (Figure 8). At first, the simplified model Ni(dmpe) was thought to cause the error in the relative energy. Therefore, the (dippe)Ni analogues **3** and **2a** were also optimized with DFT calculations. The energy difference between **3** and **2a** decreased to 3.4 kcal/mol in the gas phase, 3.6 kcal/mol in benzene, and only 1.4 kcal/mol in THF. The C−CN activation product **3** was still uphill in energy compared to the C−S activation product **2a**. The reason for this inconsistency is not clear, but the trend indicates that **3** is approaching the same energy as **2a**.

It is worthwhile to examine the calculated transition states for C−S and C−C cleavage. The two transition states for C−S cleavage, **TS2a5a** and **TS2b7b**, show completely formed Ni−C and Ni−S bonds, within 0.03 Å of their final values in **S2a** and **S2b**. The C−S bond is lengthened by 0.25 Å in **TS2a5a** and by 0.45 Å in TS**2b7b**. Consequently, the C−S bond is seen to be well along the way to being broken, especially in the kinetic product **2b**. The C−S bond is also close to lying in the NiP_2 plane (14° in **TS2a5a** and 5° in **TS2b7b**). These transition states stand in contrast to the transition state for C−CN bond cleavage. In **TS35a**, the Ni−CN and Ni−C bonds are also completely formed (within 0.05 Å of their values in **3**). The C−CN bond is stretched by only 0.14 Å, so the bond cleavage is not nearly as well progressed as in the case of the C−S cleavage. Also, the C−CN bond lies at an angle of 31° to the NiP_2 plane, similar to the value seen in the cleavage of benzonitrile (28°),[11d] and indicates that the reaction is less progressed toward the square planar product than in the case of the C−S cleavage.

One can also see why there is a kinetic preference for C−S cleavage over C−CN cleavage by examination of the HOMOs and LUMOs for the [Ni(dmpe)] fragment and the 2-cyanothiophene. As shown in Figure 9, the HOMO of the nickel is largely $d_{x^2-y^2}$, and donation into the 2-cyanothiophene LUMO would lead to population of an orbital that is C−S antibonding, thereby promoting C−S cleavage. The interaction of the 2-cyanothiophene HOMO with the [Ni(dmpe)] LUMO results in formation of complexes **S5a** and **S5b**, the η^2-C,C adducts of the thiophene that are the immediate precursors to the transition states for C−S cleavage. Both of these interactions are consistent with a kinetic preference for C−S cleavage.

Dinuclear Complexes. In the presence of excess [Ni(dippe)H]$_2$, the reaction at low temperature gave two new sets of peaks in both the ^{1}H and ^{31}P NMR spectra, with characteristics similar to those of the dinuclear complex [(dmpe)$_2$Ni$_2$(benzothiophene)] reported previously.[19b] However, crystal structures of these products could not be obtained. Therefore, DFT models of the [(dmpe)$_2$Ni$_2$(2-cyanothiophene)] complexes were constructed on the basis of the crystallographic structure of [(dmpe)$_2$Ni$_2$(benzothiophene)] (Figure 10) by changing the bridging ligand from benzothiophene to 2-cyanothiophene. Due to the asymmetric molecular structure of the 2-cyanothiophene substrate, two possible dinuclear complexes have been constructed and optimized as ground states (**S6a** and **S6b**).

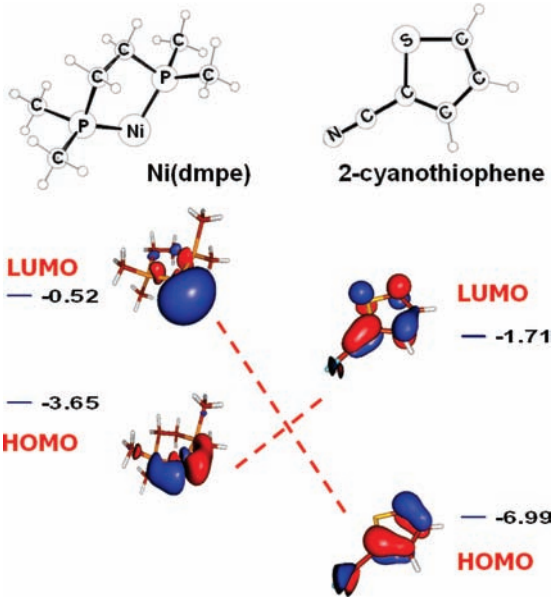

Figure 9. HOMO−LUMO interactions between [Ni(dmpe)] and 2-cyanothiophene. Energies are in eV.

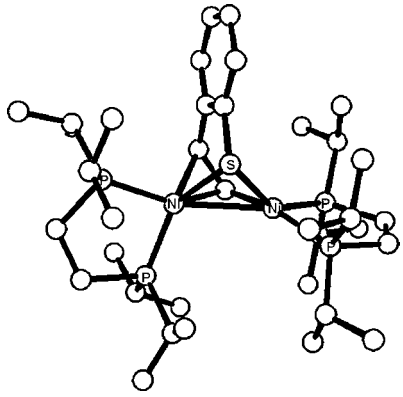

Figure 10. X-ray structure of (dippe)$_2$Ni$_2$(benzothiophene). (Reproduced with permission from ref 19b.)

Structures and selected bond lengths are shown in Figure 11 and Table 2. **S6b** is formed with Ni(dmpe) and the kinetic C−S cleavage product **S2b**, while **S6a** is formed with Ni(dmpe) and the thermodynamic C−S activation product **S2a**. Consistently, **S6a** is thermodynamically more stable than **S6b**. From the optimized structures, in each dimer there are four inequivalent phosphorus environments. For **6a**, four distinct resonances appeared in the ^{31}P NMR spectrum at low temperature (−40 °C). For **6b**, however, only one pair of doublets was observed, suggesting that there is a rapid exchange between the two nickel coordination sites that makes the two dippe ligands equivalent.[19b] This interchange has also been modeled (see movie of exchange in Supporting Information).

When [Ni(dippe)H]$_2$ was reacted with **2a** at room temperature, both **6a** and **6b** were observed and formed an equilibrium with a ratio of 3:1. Thus, the Gibbs free energy of **6b** should be about 0.6 kcal/mol higher than that of **6a**. However, using the Ni(dmpe) model, DFT calculations showed that the energy of **S6b** in THF was around 7 kcal/mol higher than that of **S6a**. Even after optimizations with the complete Ni(dippe) fragment, the energy difference between dinuclear complexes **6a** and **6b** was still 6 kcal/mol in the gas phase and 4 kcal/mol in THF. The error in energy might come from use of the model structures

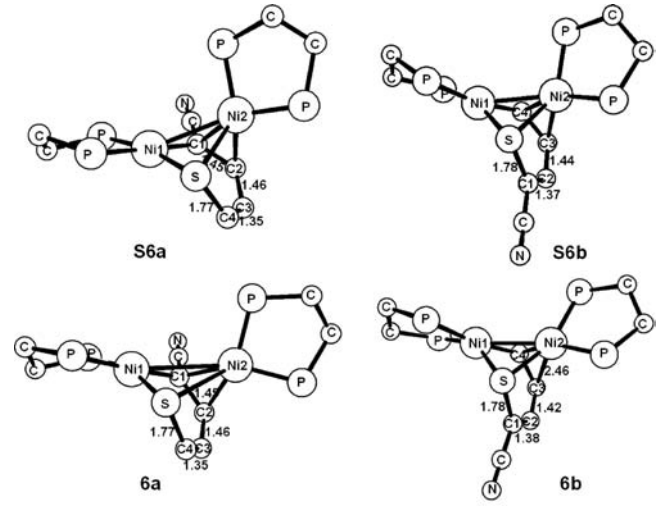

Figure 11. Optimized structures (interatomic distances in Å, angles in deg) of dinuclear complexes [(dmpe)$_2$Ni$_2$(2-cyanothiophene)] (**S6a, S6b**) and their dippe analogues (**6a, 6b**). Hydrogen atoms and isopropyl groups on the phosphorus have been omitted.

for **S6a** and **S6b**, as well as **6a** and **6b**. So far no evidence has been found to prove that the actual geometries are the same as in those in Figure 11. Three other dinuclear complexes have also been located, but all of them have much higher energies than **S6a** and **S6b** (see Supporting Information).

Conclusion

C−S bond activation occurred cleanly at room temperature when [Ni(dippe)H]$_2$ (**1**) was reacted with 2-cyanothiophene, producing a Ni metallacycle product (**2a**) where bond cleavage occurs on the nitrile-substituted side of the thiophene. When **2a** was heated in solution at 85 °C, conversion to the C−CN activated product **3** occurred, demonstrating that C−S cleavage is kinetically favored over C−C cleavage, whereas the latter is thermodynamically preferred. When the reaction was monitored at −60 °C by NMR spectroscopy, several intermediates were observed to be in equilibrium, including the isomer of **2a** in which the alternate C−S bond had been cleaved (**2b**), an η^2-C,N complex of 2-cyanothiophene (**4**), and a dinuclear adduct of **2b** (**6b**). Activation from the nonsubstituted side of the thiophene was predominant at low temperature over **2a** at −60 °C (i.e., **2b** is kinetically preferred), indicating steric contributions to the kinetic selectivity. This selectivity is similar to the previously reported reaction of 2-cyanothiophene with the analogous Pt-dippe system, which showed that cleavage of the nonsubstituted C−S bond initially predominates, but over time conversion to cleavage of the substituted C−S bond occurs as the major thermodynamic product. The Ni system mirrors this pathway (and energetics), except that the reaction is much faster than that of the Pt system. An η^2(C,N) intermediate (**4**) was also observed, comparable to that seen in analogous reactions of **1** with 2-cyanopyridine and benzonitrile, yet this species is not critical to the C−S or C−C cleavage reactions. Another intermediate seen in the low-temperature reaction was the dinuclear complex **6b**. This mixed-valent Ni(II)−Ni(0) complex was found by both experiment and theory to be more thermodynamically stable than **2a** plus [Ni(dippe)].

Independent synthesis of **6b** also led to the discovery of the regioisomer **6a**, which was not observed in the reaction of [Ni(dippe)H]$_2$ with excess 2-cyanothiophene. DFT calculations were used to model this reactivity and indicated that the greater

Table 2. Optimized Structures (Interatomic Distances in Å, Angles in Deg) and Relative Free Energies (ΔG Relative to Free Fragments, kcal/mol, PCM-Corrected in THF) of Dinuclear Complexes on the 2[Ni(dmpe)] + 2-Cyanothiophene Potential Energy Surface

	Ni1−S	Ni2−S	Ni1−Ni2	Ni1−C1	Ni1−C4	Ni2−C1	Ni2−C2	Ni2−C3	Ni2−C4	ΔG
S6b	2.264	2.462	2.650		1.902			2.254	1.968	−73.76
S6a	2.282	2.728	2.854	1.944		1.958	2.056			−80.78
6b	2.276	2.354	2.736		1.921			2.463	1.990	−64.27
6a	2.263	3.347	3.403	1.974		1.995	2.005			−68.19

ease of C−S activation over C−C activation can be attributed to a later transition state for cleavage in the latter, in which greater metal−carbon bonding is present.

Experimental Section

General Procedures. All operations were performed under a nitrogen atmosphere unless otherwise stated. The complex [Ni(dippe)H]$_2$ was prepared as previously reported.[19a] 2-Thiophenecarbonitrile (99%) was purchased from Aldrich Chemical Co., dried by stirring with sodium sulfate, and then stored under nitrogen. 2,5-Thiophenedicarbonitrile was prepared as previously reported.[24] THF-d_8 and benzene-d_6 were distilled from sodium/benzophenone prior to use. A Bruker-AXS SMART platform diffractometer equipped with an APEX II CCD detector was used for X-ray crystal structure determination. Elemental analyses were obtained from Desert Analytics. All ^{1}H, ^{31}P, and ^{13}C spectra were recorded on Bruker Avance 400 and 500 MHz spectrometers; all ^{1}H chemical shifts are reported relative to the residual proton resonance in the deuterated solvent, and ^{31}P chemical shifts are referenced relative to an 85% H_3PO_4 external standard.

Preparation of [(dippe)Ni(κ^2-S,C-SCH=CHCH=C(CN)] (2a). In a nitrogen-filled drybox, 2-cyanothiophene (5.7 μL, 0.061 mmol) was added by syringe to a J-Young NMR tube containing **1** (15.8 mg, 0.0245 mmol) in 1.5 mL of THF. The blood-red solution turned dark brown upon addition. After 12 h the solution changed to red. The THF was removed by vacuum, and the reddish-brown solid was dried by vacuum for at least 30 h to ensure removal of excess 2-cyanothiophene (19.7 mg, 0.0458 mmol, 93%). ^{1}H NMR (400 MHz, C_6D_6, 25 °C): δ 7.84 (dd, 1 H, J = 14, 7 Hz), 7.43 (t, 1 H, J = 10, 9 Hz), 6.88 (t, 1 H, J = 8 Hz), 3.12 (sextet, 2 H, J = 7 Hz), 2.05 (sextet, 2 H, J = 7 Hz), 1.28 (dd, 6 H, J = 17, 7 Hz), 1.21−0.89 (m, 4 H), 1.10 (dd, 6 H, J = 15, 7 Hz), 0.86 (m, 12 H). ^{13}C{^{1}H} NMR (126 MHz, C_6D_6, 25 °C): δ 142.46 (s), 132.64 (dd, J = 17, 4 Hz), 128.90 (d, J = 12 Hz), 120.62 (s), 113.47 (dd, J = 72, 17 Hz), 24.39 (s), 24.22 (s), 24.13 (s), 23.98 (s), 21.70 (d, J = 6 Hz), 20.49 (d, J = 20 Hz), 20.30 (d, J = 20 Hz), 19.56 (d, J = 3 Hz), 19.21 (d, J = 22 Hz), 19.10 (d, J = 21 Hz), 18.25 (s), 18.20 (s), 18.16 (s). ^{31}P{^{1}H} NMR (162 MHz, C_6D_6, 25 °C): δ73.06 (d, J = 35 Hz), 72.22 (d, J = 35 Hz). Anal. Calcd (found) for $C_{19}H_{35}NNiP_2S$: C, 53.05 (53.30); H, 8.20 (7.49); N, 3.26 (3.05).

Preparation of [(dippe)Ni(CN)(2-thiophene)] (3). In a nitrogen-filled glovebox, **2a** (20.5 mg, 0.0477 mmol) was dissolved in 1.5 mL of THF-d_8 and placed in a J-Young NMR tube. The tube was heated in an 85 °C oil bath and monitored periodically by ^{31}P NMR spectroscopy. The reaction was completed after 13 h, at which point the solvent was removed by vacuum. The residue was extracted with benzene and filtered through a plug of Celite to remove the byproduct [(dippe)Ni(CN)$_2$]. The benzene was removed by vacuum to afford a yellow solid (15.2 mg, 0.0353 mmol, 74%). ^{1}H NMR (400 MHz, C_6D_6, 25 °C): δ 7.62 (m, 1 H), 7.27 (s, 1 H), 7.03 (s, 1 H), 2.24 (sextet, 2 H, J = 7 Hz), 1.92 (sextet, 2 H, J = 7 Hz), 1.48−1.20 (m, 10 H), 0.98−0.81 (m, 18 H). ^{13}C{^{1}H} NMR (126 MHz, THF-d_8, 25 °C): δ 147.64 (dd, J = 63, 26 Hz), 131.66 (s), 128.84 (s), 127.34 (s), 125.00 (d, J = 78 Hz), 26.73 (d, J = 23 Hz), 26.56 (s), 22.74 (d, J = 19 Hz), 22.56 (d, J = 19 Hz), 21.10 (d, J = 16 Hz), 20.93 (d, J = 16 Hz), 20.52 (s), 20.15 (s), 19.71 (s), 19.23 (s), 18.27 (s). ^{31}P{^{1}H} NMR (162 MHz, THF-d_8, 25 °C): δ 85.64 (d, J = 31 Hz), 76.89 (d, J = 31 Hz). Anal. Calcd (found) for $C_{19}H_{35}NNiP_2S$: C, 53.05 (52.93); H, 8.20 (7.88); N, 3.26 (3.13).

Low-Temperature Reaction of [Ni(dippe)H]$_2$ with Excess 2-Cyanothiophene. In a drybox, **1** (9.4 mg, 0.0146 mmol) was dissolved in 1 mL of THF-d_8 and placed in an NMR tube. A septum was placed on the tube and wrapped with parafilm. The NMR tube was placed in the NMR probe and cooled to −60 °C. 2-Cyanothiophene (5.4 μL, 0.058 mmol) was dissolved in 0.1 mL of THF-d_8, the solution was drawn into a syringe, and the needle was capped with a septum to minimize the exposure to air. The solution was injected into the cold NMR tube containing **1** and immediately placed back in the probe. An initial ^{31}P NMR spectrum was taken, and subsequent spectra were taken over the course of 65 min. A steady-state equilibrium was established at this temperature between **2a**, **2b**, **4**, and **6b**. The probe was then heated to −20 °C and monitored by NMR spectroscopy over the course of 40 min, and then heated to 0 °C and monitored by NMR spectroscopy over the course of 90 min. Observed changes are described in the text, and data are given below.

[(dippe)Ni(κ^2-S,C-SC(CN)=CHCH=CH] (2b). 2b was observed at −60 °C by ^{31}P NMR spectroscopy, where it was present in a 2:1 ratio over **2a**. When the reaction temperature was raised to −20 °C, **2b** started to decrease in the reaction mixture. By the time the probe temperature had been raised to 0 °C, **2b** was no longer present. ^{31}P{^{1}H} NMR (162 MHz, THF-d_8, −60 °C): δ 85.29 (d, J = 23 Hz), 74.91 (d, J = 23 Hz).

[(dippe)Ni(η^2-C,N-2-cyanothiophene)] (4). 4 was observed at −60 °C by ^{31}P NMR spectroscopy as a significant component in the mixture. When the probe temperature was raised to −20 °C, **4** began to be consumed slowly. Consumption was more rapid when the temperature was raised to 0 °C. After 95 min at 0 °C only a small amount of **4** remained. ^{31}P{^{1}H} NMR (162 MHz, THF-d_8, −60 °C): δ 79.99 (d, J = 62 Hz), 68.73 (d, J = 62 Hz).

[(dippe)Ni]$_2$(μ-κ^2:η^3-1-cyanobutadienylthiolate)] (6b). 6b was observed at −60 °C by ^{1}H and ^{31}P NMR spectroscopy. It was not consumed as the probe temperature was raised to 0 °C. At room temperature it was consumed completely to give **2a** as the only product. ^{1}H NMR (400 MHz, THF-d_8, −20 °C): δ 7.51 (d, J = 7 Hz, H_C), 5.68 (m, J_{H-H} = 8 Hz, J_{P-H} = 18 Hz, H_A), 4.76 (m, J_{H-H} = 7,8 Hz, H_B). The coupling constants were assigned by ^{1}H{^{31}P}experiments. ^{31}P{^{1}H}NMR (162 MHz, THF-d_8, −20 °C): δ 69.27 (d, J = 17 Hz), 61.46 (d, J = 17 Hz).

(dippe)Ni(η^2-C,C-2-cyanothiophene) (5a). 5a was a very minor complex which was observed at −60 °C at the start of the low-temperature reaction. It was assigned as a Ni(0) complex because of its large P−P coupling constant (J = 75 Hz). It was short-lived and disappeared after 10 min at −60 °C. ^{31}P{^{1}H}NMR (162 MHz, THF-d_8, −60 °C): δ 64.16 (d, J = 75 Hz), 60.03 (d, J = 75 Hz).

Reaction Producing Isomeric Forms of [(dippe)Ni]$_2$(μ-κ^2:η^3-C,S-Cyanobutadienylthiolate) (6a,b)). 2a (24.0 mg, 0.0558 mmol) was dissolved in 1 mL of THF-d_8 and added to a weighed sample of **1** (26.3 mg, 0.0408 mmol). The dark reddish-brown solution was transferred to a J-Young NMR tube. The reaction was complete after 0.5 h, as confirmed by ^{31}P and ^{1}H NMR spectroscopies. The ratio of **6a**:**6b** was approximately 3:1 at room temperature. Data for **6b** are reported above. For [(dippe)Ni]$_2$(μ-κ^2:η^3-C,S-4-cyanobutadienylthiolate)] (**6a**), ^{1}H NMR (400 MHz, THF-d_8, 22 °C): δ 7.08 (t, J = 6 Hz, H_D), 5.35 (d, J = 7 Hz, H_F), 4.25 (d, J = 5 Hz, H_E). ^{31}P{^{1}H}NMR (162 MHz, THF-d_8, 25 °C): δ 69.35 (br s), 59.25

(24) Suzuki, H.; Iwao, T.; Sugiyama, T. *Bull. Inst. Chem. Res., Kyoto Univ.* **1974**, *52*, 561.

(br s). When the probe temperature was lowered to −40 °C for 25 min, four broad peaks were then observed. $^{31}P\{^1H\}$NMR (162 MHz, THF-d_8, −40 °C): δ 77.50 (br s), 64.50 (br s), 59.50 (br s), 51.8 (br s). ^{13}C NMR data for **6b** and **6a**: The alkyl region of the spectrum is indecipherable due to the multiple overlapping resonances and the presence of **1**, **6b**, and **6a** in the sample. The sp^2 resonances are distinct. $^{13}C\{^1H\}$ NMR (126 MHz, THF-d_8, 25 °C): δ 147.21 (s), 144.92 (s), 133.24 (s), 128.70 (s), 122.60 (s), 118.35 (t, J = 7 Hz), 97.80 (s), 96.56 (s), 83.55 (s), 80.71 (m).

Preparation of (dippe)Ni(κ^2-C,S-2,5-dicyanothiophene) (2c). In a nitrogen-filled glovebox, 2,5-thiophenedicarbonitrile (6.6 mg, 0.049 mmol) was dissolved in 1.5 mL of THF-d_8 and added to **1** (14.5 mg, 0.0225 mmol). The solution was placed in a J-Young NMR tube and shaken to ensure proper mixing. The reaction was monitored by ^{31}P and ^1H NMR spectroscopies and judged to be complete after 1 day. The THF was evaporated under vacuum, and the solid was dissolved in benzene and eluted through a plug of Celite. The solution was concentrated to approximately 1 mL, layered with pentane, and placed in a −30 °C freezer overnight. The liquid was removed by pipet to leave a red-orange solid (12.1 mg, 0.0266 mmol, 59%). ^1H NMR (400 MHz, THF-d_8, 25 °C): δ 7.26 (m, 1 H), 7.13 (d, 1 H, J = 7 Hz), 3.04 (sextet, 2 H, J = 7 Hz), 2.44 (sextet, 2 H, J = 7 Hz), 2.03−1.84 (m, 4 H), 1.38−1.12 (m, 24 H). $^{13}C\{^1H\}$ NMR (126 MHz, THF-d_8, 25 °C): δ 142.45 (s), 130.88 (s), 121.87 (dd, J = 69, 20 Hz), 120.38 (d, J = 5 Hz), 111.06 (s), 110.94 (s), 21.88 (d, J = 5 Hz), 21.49 (d, J = 26 Hz), 21.32 (d, J = 26 Hz), 20.05 (d, J = 2 Hz), 19.78 (d, J = 23 Hz), 19.65 (d, J = 24 Hz), 18.71 (s), 18.58 (d, J = 5 Hz). $^{31}P\{^1H\}$ NMR (162 MHz, THF-d_8, 25 °C): δ 76.76 (d, J = 37 Hz), 75.58 (d, J = 37 Hz). Anal. Calcd (found) for $C_{20}H_{34}N_2NiP_2S$: C, 52.77 (52.45); H, 7.53 (6.83); N, 6.15 (5.83).

Preparation of [(dippe)$_2$Ni$_2$(η^2-C,S-2,5-dicyanothiophene)] (6c). In a nitrogen-filled glovebox, 2,5-thiophenedicarbonitrile (5.0 mg, 0.038 mmol) was dissolved in 1.5 mL of THF-d_8 and added to **1** (24.2 mg, 0.0376 mmol). The black solution was placed in a J-Young NMR tube and shaken to ensure proper mixing. After 2.5 h, the reaction was judged to be complete by ^{31}P and ^1H NMR spectroscopies. The THF was removed by vacuum, and the crystalline black solid was dried for several hours (29 mg, 0.037 mmol, 99%). ^1H NMR (400 MHz, THF-d_8, 25 °C): δ 7.81 (d, 1 H, J = 7 Hz), 4.93 (br s), 2.78 (m, 2 H), 2.44 (m, 2 H), 2.18 (m, 4 H), 1.51−0.94 (br m, 54 H). $^{13}C\{^1H\}$ NMR (126 MHz, THF-d_8, 25 °C): δ 157.05 (s), 148.52 (s), 135.91 (s), 122.28 (s), 99.36 (s), 77.77 (s), 26.56 (s), 24.79 (d, J = 13 Hz), 22.10 (d, J = 7 Hz), 21.86 (s), 21.68 (s), 21.53 (s), 20.23 (d, J = 6 Hz), 19.87 (s), 19.65 (s), 19.50 (s), 19.17 (d, J = 5 Hz), 18.76 (s), 18.65 (s). $^{31}P\{^1H\}$ NMR (126 MHz, THF-d_8, 25 °C): δ 69.06 (br s), 59.03 (br s). Anal. Calcd (found) for $C_{34}H_{66}N_2Ni_2P_4S$: C, 52.61 (52.67); H, 8.57 (8.02); N, 3.61 (3.60).

Computational Details. When available, known experimental structures for the complexes were used as the starting point for the calculations. To simplify these calculations, the *i*-Pr groups were substituted by methyl groups. This simplification is assumed to have no steric outcome on the calculations, and in selected cases, full optimization with the dippe ligand was performed. The gas-phase structures were fully optimized in redundant internal coordinates,[25] with density functional theory (DFT) and a wave function incorporating Becke's three-parameter hybrid functional (B3),[26] along with the Lee−Yang−Parr correlation functional (LYP).[27] All calculations were performed using the Gaussian03[28] package. The Ni and P atoms were represented with the effective core pseudopotentials of the Stuttgart group and the associated basis sets improved with a set of f-polarization functions for Ni (α = 3.130)[29] and a set of d-polarization functions for P (α = 0.387) and S (α = 0.503).[30] The remaining atoms (C, H, and N) were represented with 6-31G(d,p)[31] basis sets. The geometry optimizations were performed without any symmetry constraints, and the local minima and the transition states were checked by frequency calculations. For each transition-state structure, the intrinsic reaction coordinate (IRC) routes were calculated in both directions toward the corresponding minima. Movies showing these motions are included in the Supporting Information. For some of the transition states, the IRC calculations failed to reach the energy minima on the potential energy surface; therefore, in those cases geometry optimizations were carried out as a continuation of the IRC path. Because of the polarity of the structures, the solvent effects on their relative stabilities were evaluated by calculating the free energies of solvation in terms of the polarizable continuum model (PCM).[9] Self-consistent reaction field (SCRF) calculations using the PCM-UA0 solvation model[32] were carried out for the gas-phase optimized structures. The dielectric constant in the PCM calculations was set to ϵ = 7.58 to simulate THF and ϵ = 2.247 to simulate benzene as the solvent media used in the experimental study. The energies discussed in the potential energy surface plot are Gibbs free energies, which have been calculated at 298.15 K and 1 atm. The ORTEP32 package was used to display the molecular structures.

Acknowledgment. Financial support from the National Science Foundation (CHE-0717040) for the experimental work (M.R.G.) and from the U.S. Department of Energy (grant FG02-86ER13569) for the calculational work (T.L.) is gratefully acknowledged.

Supporting Information Available: Table of distribution of species for the low-temperature reaction; complete ref 28; figure showing energies of calculated species in gas phase and benzene; pictures of molecular orbitals; calculated coordinates; results with additional basis sets; X-ray diffraction details (in CIF format) for **2a**, **3** (two morphologies), and **2c**; and five movies showing the IRC calculated reaction paths. This material is available free of charge via the Internet at http://pubs.acs.org. The structures are also deposited in the Cambridge Crystallographic Database as CCDC Nos. 774682−774685.

JA104158H

(25) Peng, C.; Ayala, P. Y.; Schlegel, H. B.; Frisch, M. J. *J. Comput. Chem.* **1996**, *17*, 49.
(26) Becke, A. D. *J. Chem. Phys.* **1993**, *98*, 5648.
(27) Lee, C.; Yang, W.; Parr, R. G. *Phys. Rev. B* **1988**, *37*, 785.
(28) Frisch, M. J.; et al. *Gaussian03*; Gaussian, Inc.: Wallingford, CT, 2004.
(29) Ehlers, A. W.; Bohme, M.; Dapprich, S.; Gobbi, A.; Hollwarth, A.; Jonas, V.; Kohler, K. F.; Stegmann, R.; Veldkamp, A.; Frenking, G. *Chem. Phys. Lett.* **1993**, *208*, 111.
(30) Hollwarth, A.; Bohme, M.; Dapprich, S.; Ehlers, A. W.; Gobbi, A.; Jonas, V.; Kohler, K. F.; Stegmann, R.; Veldkamp, A.; Frenking, G. *Chem. Phys. Lett.* **1993**, *208*, 237.
(31) Hehre, W. J.; Ditchfield, R.; Pople, J. A. *J. Chem. Phys.* **1972**, *56*, 2257.
(32) Barone, V.; Cossi, M.; Tomasi, J. *J. Chem. Phys.* **1997**, *107*, 3210.